

Pulsed ELDOR Spectroscopy Measures the Distance between the Two Tyrosyl Radicals in the R2 Subunit of the *E. coli* Ribonucleotide Reductase

Marina Bennati,^{*,†} Axel Weber,[†] Jelena Antonic,[‡] Deborah L. Perlstein,[‡] John Robblee,[‡] and JoAnne Stubbe[‡]

Institute of Physical and Theoretical Chemistry, J. Goethe University of Frankfurt, D-60439 Frankfurt, Germany, and Departments of Chemistry and Biology, Massachusetts Institute of Technology, Cambridge, Massachusetts 02139-4307

Received May 19, 2003; E-mail: bennati@chemie.uni-frankfurt.de

Escherichia coli ribonucleotide reductase (RNR) catalyzes the conversion of nucleoside diphosphates (NDPs) to deoxynucleoside diphosphates (dNDPs). This RNR is composed of two homodimeric subunits: R1 and R2.¹ R1 binds the NDPs in an active site with three essential cysteines and houses the binding sites for the allosteric effectors that govern turnover and specificity. R2 harbors the essential di-iron tyrosyl radical (Y^*) cofactor. The mechanism of nucleotide reduction has been extensively studied,² and structures of R1^{3,4} and of R2^{5,6} are available. Despite this wealth of information, a major unresolved issue is the mechanism of radical initiation: how the Y^* on R2 generates a transient thiyl radical on R1 over a 35 Å distance based on a docking model of a 1:1 complex of R1 and R2.⁷

Pulsed electron–electron double resonance (PELDOR) is a method that monitors weak dipole–dipole interactions between the electron spins of radicals that span distances between approximately 15 and 80 Å.^{8–10} This method could provide a means to measure the distance between the active site of R1 and Y^* on R2 if a paramagnetic species could be specifically attached to one of the cysteines within R1. As proof of concept, we have used PELDOR to make the first direct measurement of the distance between the Y^* 's on each monomer of R2, as in the crystal structure of R2⁵ the Y^* 's are reduced and consequently R2 is inactive. This method also provides the first direct evidence for two Y^* 's within a single R2 homodimer, giving insight into the distribution of Y^* on R2.

Pulsed ELDOR spectroscopy is based on the DEER (double electron–electron resonance) two-frequency pulse sequence.^{8,11} We now report experiments using an improved version of the original sequence, a four-pulse DEER sequence,¹² that allows a more precise determination of the dipolar spectrum and of the modulation depth parameter λ via a dead-time free detection. The four-pulse DEER sequence was applied to samples of *E. coli* R2 containing 1.07 Y^* 's and ranging in concentration from 0.23 to 2.3 mM (for sample characterization, see Supporting Information). A control experiment was carried out using the active *Saccharomyces cerevisiae* subunit (Rnr2Rnr4) containing 0.6 Y^* located uniquely on the Rnr2 monomer.¹³

Figure 1A displays the echo detected EPR absorption of Y^* and (1B) four-pulse DEER echo modulation traces of Y^* from *E. coli* R2 (0.23 mM) recorded with an X-band Bruker ELEXSYS E580 spectrometer with ELDOR capability.¹⁴ The time traces (1B) show an oscillation superimposed on an echo decay, which are typical features of PELDOR data.^{9,10} For an estimate of the oscillation frequency, the echo decay was fitted with a monoexponential function and subtracted from the data set. Subsequent Fourier transformation (FT) led to the frequency spectrum Figure 1C, as illustrated for the trace (a) in Figure 1B.

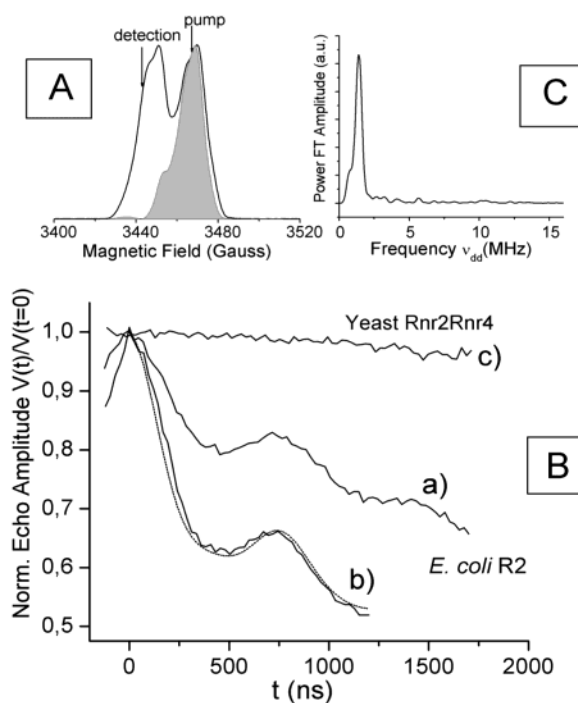


Figure 1. (A,B,C) DEER traces of a 0.23 mM solution of R2 from *E. coli* and of a 0.31 mM solution of Rnr2Rnr4 from yeast. (1A) Spin-echo detected spectrum of the Y^* in R2 from *E. coli* at 5 K. The visible doublet arises from the hfc to one β -methylene proton. The arrows indicate the position of the pump and detection frequencies with $\Delta\nu = 70$ MHz. The shaded area illustrates the calculated excitation profile for an ideal π -pump pulse of 12 ns. (1B) Time traces (V_i) normalized with the echo signal intensity at zero time, that is, the time point where pump pulse and primary echo are coincident. All pulses on the detection frequency ($\pi/2-\pi-\pi$) were 32 ns; τ (spacing between $\pi/2$ and π -pulse) = 160 ns; $T = 5$ K; 12 h acquisition time. For the *E. coli* RNR trace (a) and yeast RNR (c): $t_{\text{pump}} = 32$ ns. For the *E. coli* RNR trace (b): $t_{\text{pump}} = 12$ ns. Dotted line: simulation using a model for diluted spin pairs as explained in the text. (1C) Fourier transformation of trace (a) in (1B) after subtraction of a monoexponential decay, Hamming filtering, and zero-filling.

The spectrum displays one peak centered at 1.39 ± 0.05 MHz that we interpret as the singularity ($\theta = 90^\circ$) of a dipolar powder pattern. Because we expect the Y^* 's to be at a distance of at least 30 Å,⁵ exchange interactions are negligible¹⁰ and the modulation frequency ν_{dd} of an isolated spin pair AB is related to their interspin distance r_{AB} by the expression for the dipolar coupling in the high-field approximation:¹⁵

$$\nu_{\text{dd}} = \frac{\mu_0 \mu_{\text{B}}^2 g_{\text{A}} g_{\text{B}} (3 \cos^2 \theta - 1)}{4\pi h r_{\text{AB}}^3} \quad (1)$$

[†] J. Goethe University of Frankfurt.

[‡] Massachusetts Institute of Technology.

This approximation is usually valid for paramagnetic systems at X-band when g -anisotropy is small.^{9,10} In our case, the g -anisotropy is not resolved (see Figure 1A), and we use the average g value of 2.005¹⁶ for both g_A and g_B . Using this model, we determined that the experimentally observed dipolar frequency of 1.39 ± 0.05 MHz results in a point–dipole distance of 33.5 ± 0.4 Å. The error arises mainly from the determination of ν_{dd} by the FT analysis, specifically by the subtraction of the echo decay function.

Because no pulsed ELDOR experiments have been previously performed on any class I RNR, care was taken to establish that the echo modulation observed arises from intramolecular Y^* interactions within an R2. First, if the modulation effect were caused by Y^* 's on different R2's, then the modulation frequency should be dependent on the protein concentration, as the average distance between R2's in a homogeneously distributed solution decreases with increasing protein concentration. We therefore recorded the modulation traces at several R2 concentrations (0.23, 0.57, and 2.3 mM, Supporting Information). No changes in the modulation frequency were observed, indicating that the observed oscillation is due to intramolecular interactions.

Second, effects from hyperfine coupling (ESEEM) must also be excluded as a basis of the echo modulation. These effects are usually strongly attenuated if the pump and detecting frequencies are not coherent, as in this case. Furthermore, because hyperfine interactions are local, they should also be visible in R2 samples containing only one Y^* . An experiment with the yeast Rnr2Rnr4 (0.31 mM) was carried out to eliminate the possibility that the modulations observed (Figure 1B) are caused by hyperfine interactions. The four-pulse DEER experiment under experimental conditions identical to those with *E. coli* R2 is displayed in Figure 1B (c) and clearly shows no modulation. This experiment unambiguously demonstrates that the echo modulation effect observed in *E. coli* R2 arises from a dipolar interaction between Y^* 's on a single R2.

We have performed simulations assuming that the Y^* radical pairs in R2 are located at a well-defined distance and orientation relative to one another and that their conformational distribution within R2 is negligible. Using this assumption, we have calculated the time traces according to the model for diluted spin pairs, where $V(t)$ is described as a product of an intramolecular contribution (V_{intra}) from the isolated spin pairs and an intermolecular contribution (V_{inter}) from the homogeneous distribution of the radicals in solution⁹ (Supporting Information). In Figure 1B, we display a simulation of the trace (b) which leads to the parameters $\lambda = 0.25$, $\nu_{\text{dd}} = 1.44$ MHz; consequently, $r = 33.1$ Å. The error in ν_{dd} is estimated ≤ 0.03 MHz, giving an error in the distance of ≤ 0.2 Å.

The distance $r = 33.1 \pm 0.2$ Å has now to be related to the spin density distribution on Y^* and to the distance and orientation of the Y^* pair. In previous work,^{17,18} the point–dipole interaction between delocalized radicals at long distances ($r \geq$ approximately 25 Å) was interpreted as between the center of gravity of the spin density. Accordingly, the center of gravity for the spin density on Y^* in R2¹⁹ is located on the axis connecting the ring center and the aromatic C4, resulting in a distance of 32.6 Å based on the recent R2 crystal structure at 1.4 Å resolution.⁶ This value agrees well with the determined effective point–dipole distance of 33.1 Å. However, we point out that the observed dipolar coupling results as a sum of the individual dipolar interactions at the different spin density sites. Performing this summation using the coordinates from ref 6, we calculate an effective dipolar coupling of 1.53 MHz as compared to 1.44 MHz from the PELDOR analysis. The close agreement verifies that the structure in the crystal (with reduced Y122's, pH 6) is similar to that in solution (pH 7.6).

Finally, we note that the modulation depth gives insight into the population of the Y^* pairs as it is directly proportional to the fraction of excited spins and the fraction of radical pairs.^{9,10} The determined value $\lambda = 0.25$ indicates that at least 25% of the Y^* 's are paired. Further, we expect that the population of the pairs is larger than 0.25 due to the partial excitation of the Y^* 's by the pump pulse (Figure 1A). A precise determination is in progress using a calibration of λ with standards.

In conclusion, the reported PELDOR experiments have demonstrated that this method will be useful in determining the distance between the R1 active site and the Y^* in R2, as the active site of R1 can be specifically labeled using a number of mechanism-based inhibitors that generate well-characterized organic radicals. The distance between these two active sites is a critical piece of information in thinking about long-range radical initiation in class I RNRs. Efforts are underway to make this measurement using 2'-azido-2'-deoxynucleotide, a stoichiometric inhibitor that generates a nitrogen-centered radical covalently bound to Cys 225 and the nucleotide in the active site of R1.²⁰

Acknowledgment. Prof. T. F. Prisner is acknowledged for financial support and discussions. O. Schiemann is thanked for donating nitroxide biradicals to calibrate the PELDOR sequences.

Supporting Information Available: Materials, concentration dependence, and simulation model (PDF). This material is available free of charge via the Internet at <http://pubs.acs.org>.

References

- Jordan, A.; Reichard, P. *Annu. Rev. Biochem.* **1998**, *67*, 71.
- Licht, S.; Stubbe, J. Mechanistic Investigations of Ribonucleotide Reductases. In *Comprehensive Natural Products Chemistry*; Barton, S. D., Nakanishi, K., Meth-Cohn, O., Poultier, C. D., Eds.; Elsevier Science: New York, 1999; Vol. 5, p 163.
- Uhlin, U.; Eklund, H. *J. Mol. Biol.* **1996**, *262*, 358.
- Eriksson, M.; Uhlin, U.; Ramaswamy, S.; Ekberg, M.; Regnstrom, K.; Sjöberg, B. M.; Eklund, H. *Structure* **1997**, *5*, 1077.
- Nordlund, P.; Sjöberg, B.-M.; Eklund, H. *Nature* **1990**, *345*, 593.
- Högbom, M.; Galander, M.; Andersson, M.; Kolberg, M.; Hofbauer, W.; Lassmann, G.; Nordlund, P.; Lendzian, F. *Proc. Natl. Acad. Sci. U.S.A.* **2003**, *100*, 3209.
- Uhlin, U.; Eklund, H. *Nature* **1994**, *370*, 533.
- Milov, A. D.; Ponomarev, A. B.; Tsvetkov, Y. D. *Chem. Phys. Lett.* **1984**, *110*, 67.
- Milov, A. D.; Maryasov, A. G.; Tsvetkov, Y. D. *Appl. Magn. Reson.* **1998**, *15*, 107.
- Jeschke, G. *Macromol. Rapid Commun.* **2002**, *23*, 227.
- Larsen, R. G.; Singel, D. J. *J. Chem. Phys.* **1993**, *98*, 5134.
- Pannier, M.; Veit, S.; Godt, A.; Jeschke, G.; Spiess, H. W. *J. Magn. Reson.* **2000**, *142*, 331.
- In yeast there are two genes for the small subunit Rnr2 and Rnr4. Expression of these genes gives a homodimer of Rnr2 and a homodimer of Rnr4. Recent studies in vitro (Ge, J.; Perlstein, D. L.; Nguyen, H. T.; Bar, G.; Griffin, R. G.; Stubbe, J. *Proc. Natl. Acad. Sci. U.S.A.* **2001**, *98*, 10067–10072. Chabes, A.; Domkin, V.; Larsson, G.; Liu, A.; Gräslund, A.; Wijmenga, S.; Thelander, L. *Proc. Natl. Acad. Sci. U.S.A.* **2000**, *97*, 2474–2479) and in vivo (Yao, R.; Zhang, Z.; Buccini, B.; Perlstein, D. L.; Stubbe, J.; Huang, M. *Proc. Natl. Acad. Sci. U.S.A.* **2003**, *100* (11), 6628–6633) have suggested that the active small subunit in yeast is a heterodimer containing one monomer of Rnr2 and one monomer of Rnr4. Rnr4 is essential for di-iron Y^* assembly in Rnr2. However, Rnr4 lacks three conserved ligands to the metal center that precludes formation of any cofactor.
- Weber, A.; Schiemann, O.; Bode, B.; Prisner, T. F. *J. Magn. Reson.* **2002**, *157*, 277.
- θ is the angle between the magnetic field B_0 and the distance vector r_{AB} ; μ_B is the Bohr magneton; h is the Planck constant and g_A and g_B are the g values of the unpaired electrons A and B.
- Gerfen, G. J.; Bellew, B. F.; Un, S.; Bollinger, J. M., Jr.; Stubbe, J.; Griffin, R. G.; Singel, D. J. *J. Am. Chem. Soc.* **1993**, *115*, 6420.
- Astashkin, A. V.; Kodera, Y.; Kawamori, A. *Biochim. Biophys. Acta* **1994**, *1187*, 89.
- Bittl, R.; Zech, S. *J. Phys. Chem. B* **1997**, *101*, 1429.
- Honganson, C. W.; Sahlín, M.; Sjöberg, B.-M.; Babcock, G. T. *J. Am. Chem. Soc.* **1996**, *118*, 4672.
- (a) Sjöberg, B.-M.; Gräslund, A.; Eckstein, F. *J. Biol. Chem.* **1983**, *258*, 8060. (b) van der Donk, W. A.; Stubbe, J.; Gerfen, G. J.; Bellew, B. F.; Griffin, R. G. *J. Am. Chem. Soc.* **1995**, *117*, 8908.

JA0362095